Aerosol Science and Technology 33:440–454 (2000)

Published by Taylor and Francis
0278-6826/00/$12.00 + .00

Evaluation of the Fractal Properties of Cluster–Cluster Aggregates

A. M. Brasil, T. L. Farias, and M. G. Carvalho*
DEPARTMENT OF MECHANICAL ENGINEERING, INSTITUTO SUPERIOR TÉCNICO,
1049-001 LISBON, PORTUGAL

ABSTRACT. While the fractal dimension of cluster–cluster aggregates, D_f, appears to be a well-established property, the fractal prefactor, k_g (also known as structural coefficient), continues to exhibit a large range of possible values. In the present paper, an attempt is made to clarify this issue which leads to conclusive results concerning the value to adopt for the fractal prefactor of simulated aggregates. Starting from a large population of "free" numerically simulated aggregates (i.e., where no restrictions to aggregate formation were imposed) the fractal properties obtained were estimated both using morphological concepts as well as light scattering theories. Furthermore, studies for aggregates having predefined morphological k_g values (namely, $k_g > 2$ and ca. 1) were also performed in order to check the viability of these values. The results obtained for the three different populations of aggregates considered were used to infer, through a best-fit analysis, the fractal properties. Our best estimates are $k_g \approx 1.27$ and $D_f \approx 1.82$, which are approximately independent of aggregate size and composition. These results are in very good agreement with numerical predictions reported by previous authors. However, experimental results systematically indicate $k_g > 2$. This motivated the present authors to identify possible reasons for these large discrepancies. Present calculations indicate that partial sintering in conjunction with the polydispersity of aggregates (resulting in a cut-off function coefficient, k_p, >1) contributes to a systematic increase in k_g, possibly justifying the differences between numerical and experimental results.

INTRODUCTION

Aggregated particles, such as aerosols, are present in a wide range of engineering fields such as combustion processes for power generation and pigment production. These agglomerates are usually composed of fine primary particles that coagulate to form irregular clusters. Because of complex nucleation and aggregation processes, most combustion generated agglomerates have a broad size distribution (see Köylü and Faeth 1992; Megaridis and Dobbins 1990 and references cited therein). Although different in their size, shape, radius of gyration, and particle density, these aggregates exhibit complex geometry that fortunately can be characterized as mass fractals; that is, the number of primary

* Corresponding author.

particles per aggregate, N, scales with the radius of gyration, R_g, as follows:

$$N = k_g(R_g/a)^{D_f}, \quad (1)$$

where k_g is the fractal prefactor (also known as the structural coefficient), D_f is the fractal dimension, and a is the primary particle radius. Most studies in the past have considered the fractal dimension as the key property to characterize fractal-like aggregates. However, Wu and Friedlander (1993), Cai et al. (1995), Köylü et al. (1995a), and Sorensen and Roberts (1997) have shown that both the fractal dimension and the prefactor must be correctly known in order to fully define the fractal structure of a specific aggregate. This seems reasonable from Equation 1, which indicates that the fractal dimension alone is not sufficient to determine the radius of gyration of an aggregate assuming that the radius of the monomers and the number of monomers within the aggregate are known.

The fractal dimension has received its deserved attention from the scientific community, and conclusive values for this property have been achieved. Megaridis and Dobbins (1990) have unified most of the experimental and computational results obtained for the fractal dimension of soot, silica, and carbon black particles, among other types of materials. Apart from singular results, most predictions fall within the range of 1.6–1.9. More recently, Köylü and Faeth (1994a,b) and Köylü et al. (1995a,b, 1997) have confirmed these values numerically and experimentally both through image analysis and light scattering predictions of soot and alumina particles. Brasil et al. (1999) and Oh and Sorensen (1997, 1998) have also produced numerical aggregates that lead to D_f in the range of 1.7–1.9, therefore confirming the range previously presented. Table 1 summarizes the most relevant results obtained by independent authors for the fractal dimensions.

Contrasting with the amount of studies concerning D_f, the fractal prefactor was either ignored or considered as a second class fractal property by most researchers in past years.

TABLE 1. Fractal dimension and fractal prefactor reported by several authors.

Authors	Method	k_g	D_f
Mountain and Mulholland (1988)	CS	1.59	1.69
Meakin (1984)	CS	1.05	1.74
Mountain and Mulholland (1988)	CS	1.37	1.82
Wu and Friedlander (1993)	CS	1.30	1.84
Köylü et al. (1995b)	ALS	2.25	1.86
Köylü et al. (1995b)	ALS	2.78	1.75
Köylü et al. (1995b)	3-D TEM	2.71	1.65
Köylü et al. (1995b)	2-D TEM	2.39	1.67
Köylü et al. (1995b)	2-D TEM	2.35	1.66
Köylü et al. (1995b)	2-D TEM	2.17	1.73
Köylü et al. (1995b)	2-D TEM	2.18	1.54
Puri et al. (1993)	ALS	3.50	1.40
Cai et al. (1995)	3-D TEM	1.23	1.74
Cai et al. (1995)	2-D TEM	2.45	1.74
Samson et al. (1987)	3-D TEM	3.49	1.40
Samson et al. (1987)	2-D TEM	2.67	1.47
Megaridis and Dobbins (1990)	2-D TEM	2.18	1.62
Megaridis and Dobbins (1990)	2-D TEM	1.80	1.74
Present results	CS	1.27	1.82

ALS = angular light scattering.
CS = computer simulation.
3-D = three-dimensional analysis.
2-D = projected images.
TEM = transmition electron microscope.

However, according to Equation (1), from the point of view of fully characterizing fractal-like aggregates it is necessary to establish values both for D_f and k_g. Unfortunately, the selection of universal values for the fractal prefactor for cluster–cluster (as well as particle–cluster) aggregates is still a controversial issue. Wu and Friedlander (1993) and, more recently, Köylü et al. (1995a) have unified most of the experimental and numerical data reported on this property (also included in Table 1). For example, for cluster–cluster aggregates results published in the literature for k_g indicate values between 1.23 (Cai et al. 1995) and 3.47 (Samson et al. 1987). The range of results published varies by more than 200%, indicating that this issue deserves more attention. In spite of the range of values published, it was noted that results based on

numerically simulated aggregates are systematically inferior to k_g values inferred from experimental data. An exception to this trend has been presented by Cai et al. (1995) when analyzing the structure of soot particles extracted from a premixed methane/oxygen flame obtaining $D_f = 1.74$ and $k_g = 1.23$ (see Table 1).

Based on the previous considerations, the main objective of the present paper was to identify a possible universal value for the fractal prefactor of cluster–cluster aggregates. In order to achieve this objective, the following approach was adopted:

1. A large population of "free" cluster-cluster aggregates (ca. 256) was numerically simulated using computer software previously used by several authors (Farias et al. 1995; Brasil et al. 1999; Köylü et al. 1995b). Aggregates were built without any restrictions concerning fractal dimensions. Results obtained for the D_{fM} and k_{gM} (referred to as morphological properties hereafter) were then estimated through Equation (1) for the whole population.
2. Light scattering predictions were estimated for the simulated aggregates using typical values for the primary particle sizes and complex refractive indices for organic (e.g., soot) and inorganic (e.g., alumina) combustion generated particles. Plotted in a proper manner, light scattering predictions also indicate the fractal dimension and prefactor of the aggregates. Results obtained (D_{fLLS} and k_{gLLS}) were compared with the morphological predictions described in the previous point.
3. Aggregates were built restricting the fractal dimension within the expected values (ca. 1.7–1.8) and varying the prefactor. Values selected for D_f and k_g were then confirmed through Equation (1) for the whole population and compared with the ones obtained through light scattering predictions.
4. For the range of D_f and k_g covered, morphological and light scattering fractal predictions were compared and conclusions were obtained concerning the most adequate values of k_g and D_f.

Finally, an attempt was made to identify possible reasons for the large discrepancies between the experimental and numerical values reported for k_g.

The paper begins with a description of the numerical simulation procedure adopted to generate the fractal-like aggregates. The light scattering theory used to characterize the optical properties of the simulated aggregates is then described. Further on, the population of aggregates used for the present investigation is characterized, in particular, their fractal properties. An analysis of the fractal dimensions obtained for the populations using morphological and light scattering approaches follows. An attempt is then made to identify a reason for the large discrepancies between the experimental and numerical values reported for k_g. Finally, major conclusions of the present work are summarized.

NUMERICAL SIMULATION OF CLUSTER–CLUSTER AGGREGATES

Simulation of Aggregates

Various procedures to construct agglomerates composed of spherical primary units have been discussed by Jullien and Botet (1987) and Botet and Jullien (1988). These methods are based on simple algorithms that mimic cluster–cluster or particle–cluster aggregation processes due to Brownian motion. Due to their relative simplicity, several investigators (e.g., Vold 1963; Hutchinson and Sutherland 1965; Witten and Sander 1981, 1983; Meakin 1983a,b) have adopted particle–cluster methods; however, the aggregates obtained cannot be considered fractals (Jullien and Botet 1987). A more physically-based method was developed by Mountain et al. (1986), who generated soot aggregates using a numerical simulation involving cluster–cluster aggregation based on the solution of the Langevin equations. This approach yields fractal-like aggregates that satisfy the power-law

relationship of Equation (1); however, for the present study it was required that the aggregates had, when necessary, specific predefined fractal dimensions. As a result, an alternative simulation method previously used by Farias et al. (1995, 1996), Köylü et al. (1995b), and Brasil et al. (1999) was applied during the present investigation.

The aggregate simulation method involved creating a population of aggregates by cluster–cluster aggregation using a sequential algorithm that satisfies Equation (1) intrinsically, rather than performing numerical simulations based on Langevin dynamics along the lines of the approach used by Mountain et al. (1986). For prespecified values of D_f and k_g, the aggregate generation process was initiated by randomly attaching individual and pairs of particles to each other, assuming uniform distributions of the point and orientation of attachment, while rejecting configurations where primary particles intersected. Further on, if the control of the fractal dimensions, D_f and k_g, was desired, the radius of gyration of the new aggregate was calculated based on the known positions of the primary particles and checked to see if Equation (1) was satisfied for the fractal dimension and prefactor selected. This procedure was continued in order to form progressively larger aggregates that obeyed the statistical relationships of mass fractal objects. As a default a hierarchical approach was used where only clusters having the same number of primary particles (or a similar number if N was odd) were joined together (Jullien and Botet 1987). Nevertheless, if desired the model was capable of creating non-hierarchical aggregates.

In the present study we started by creating a population of aggregates where no restrictions on the fractal dimensions were imposed. Further on, while trying to check the validity of different solutions for D_f, and k_g, prespecified values were assigned. The population of simulated aggregates involved N in the range 8–1024, considering 8 different aggregate size classes and 32 aggregates per class (Figure 1 shows a log–log plot of R_g/a versus N for the population of aggregates generated). This sample size was

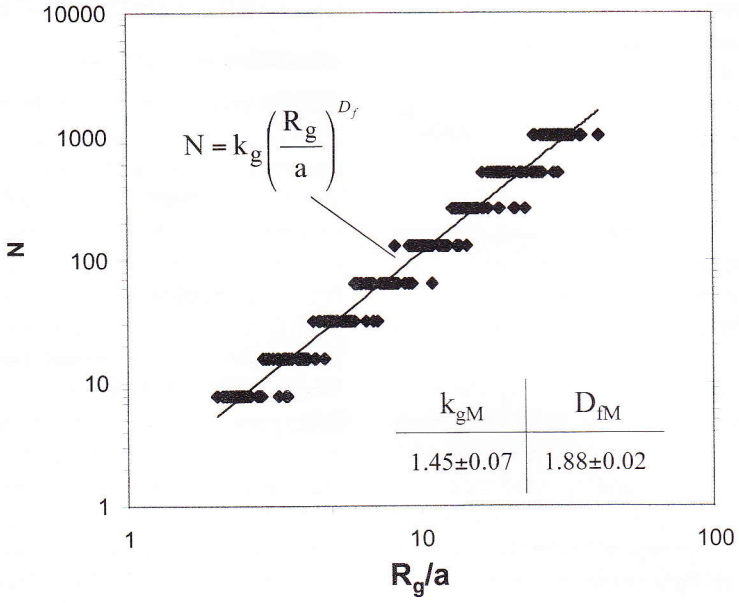

FIGURE 1. Number of particles per aggregate versus radius of gyration normalized by particle radius yielding the morphological fractal dimension and fractal prefactor for "free" simulated aggregates.

established in order to obtain a numerical uncertainty (95% confidence) $<10\%$ for the different variables investigated throughout the present study.

LIGHT SCATTERING PREDICTIONS OF AGGREGATED SPHERICAL PARTICLES

One of the earliest versions of a scattering theory for aggregates formed by small particles was developed by Jones (1979a,b) and based on the original integral equation formulation of Saxon (1974). Purcell and Pennypacker (1973) developed a similar approach to the aggregate scattering problem. Several others, including Berry and Percival (1986), Goedecke and O'Brien (1988), Draine (1988), Nelson (1989), and Iskander et al. (1989), followed these studies. More recently, Lou and Charalampopoulos (1994) presented a general form of the governing equation of the electric internal field of an assembly of particles for conditions where individual particles satisfied the Rayleigh limit. Although different in their mathematical approach, the fundamental light scattering formulations mentioned above all involve the solution of the same set of linear equations (Equation (2)) to obtain the internal electric field of the primary particles. Among them, the formulation of Lou and Charalampopoulos (1994)—denoted the Integral Equations Formulation for Scattering (IEFS)—is the most complete formulation, while the remaining formulations can be obtained by introducing simplifications in some of the terms. In addition, IEFS satisfies energy conservation required among extinction, absorption, and total scattering. Because IEFS involves no additional computational effort, it was employed in this study to compute the light scattering characteristics of the aggregates.

The Integral Equation Formulation for Scattering

The following description of this theoretical method is brief; additional details can be found in Farias et al. (1998, 1996) and Lou and Charalampopoulos (1994).

The IEFS method divides an aggregate into sufficiently small units (the primary particles) so that the internal field within each particle is assumed to be uniform. By considering not only the phase differences but also the multiple scattering and self-interaction terms, the internal electrical field of each particle, $\boldsymbol{E}_j$, is then obtained from the following system of $3N \times 3N$ linear equations:

$$\boldsymbol{E}_j = \left(\frac{3}{m^2+2}\right)\boldsymbol{E}_{inc,j} + i\left(\frac{m^2-1}{m^2+2}\right)x_p^2 j_1(x_p) \times \sum_{l=1,\neq j}^{N} \bar{\boldsymbol{T}}_{jl}\boldsymbol{E}_l + s_j\boldsymbol{E}_j;\ j = 1, 2, \ldots, N, \tag{2}$$

where $m = \eta + i\kappa$ represents the complex refractive index of each small particle; $\boldsymbol{E}_{inc} = \boldsymbol{E}_o \exp(ikz)$ represents the incident electric field propagating along the z axis with a wave number of $k = 2\pi/\lambda$; $j_1(x_p)$ is the first-order spherical Bessel function of the first kind; s_j is the self interaction term; and $\bar{\boldsymbol{T}}$ is the scattering matrix. Once the internal field of each spherical particle is known from Equation (2), various optical cross sections can be obtained for an aggregate with N uniform size particles (see, e.g., Farias et al. 1998 and references cited therein). Relevant for the present study is the vertical–vertical differential scattering cross section, C_{vv}^a, given by

$$C_{vv}^a(\theta,\phi) = \frac{1}{k^2}x_p^4 j_1^2(x_p)|m^2-1|^2 \times \left|\sum_{j=1}^{N}\exp(-ikr_j\cos\beta_j) \times (E_{j,\theta}\hat{\theta} + E_{j,\phi}\hat{\phi})_{vv}\right|^2, \tag{3}$$

where the direction of the scattered field is represented by spherical coordinates θ and ϕ (unit vectors by $\hat{\theta}$ and $\hat{\phi}$), the position of each individual unit by (r_j, θ_j, ϕ_j), the direction of polarization by subscript vv, and $\cos\beta_j = \cos\theta_j\cos\theta + \sin\theta_j\sin\theta\cos(\phi_j - \phi)$.

This property contains important information regarding the fractal nature of the aggregates.

In fact, fractals exhibit a large angle scattering regime (also known as power-law regime) in such a form that both D_f and k_g can be extracted as follows (see Julien and Botet 1987; Köylü and Faeth, 1994a,b):

$$C^a_{vv}/NC^p_{vv} = k_g k_p (qa)^{-D_f}, \text{ thus} \quad (4)$$

$$D_f = -\ln\left(C^a_{vv}/NC^p_{vv} k_g k_p\right)/\ln(qa), \quad (5)$$

$$k_g = C^a_{vv}/\left(k_p NC^p_{vv}\right) \text{ for } qa = 1, \quad (6)$$

where q is the modulus of the scattering vector ($q = (4\pi/\lambda)\sin(\theta/2)$), a the radius of the particle, k_p the cut-off function coefficient (see Sorensen and Wang 1999), and C^p_{vv} is the scattering cross section of a single particle.

In summary, on a log–log plot the slope of the normalized scattering curve obtained in the large angle regime should be equal to $-D_{fLLS}$; while the light scattering fractal prefactor, k_{gLLS}, can be inferred from the power–law slope where $qa = 1$.

The cut-off function coefficient k_p, has been ignored in the past by most researchers. Fortunately, Sorensen and Wang (1999) indicate that this coefficient is one for monodisperse aggregate populations. While in the present study only monodisperse populations have been considered, in most experimental situations this is seldom the case. For example, Köylü and Faeth (1994a,b) have shown that soot aggregate populations follow log-normal distribution functions with standard deviations > 1.5. For these types of polydisperse populations, Sorensen and Wang (1999) indicate $k_p > 1.5$. This implies that past experimental determinations of the fractal prefactor using light scattering measurements may have a systematic gap of this order of magnitude, i.e., experimental results could be over-estimated by more than 50%.

It is important to notice that the accuracy of the IEFS solutions depends on the ratio between the primary particle size and the wavelength because the approximation of uniform electric field within each primary particle starts failing when this size parameter is not considerably <1. Farias et al. (1995) state that IEFS is applicable for primary particle size parameter $x = 2\pi a/\lambda < 0.4$. Fortunately, most combustion generated aggregates fall within the nanosize particle domain with primary particle mean diameter between 10–50 nm. Therefore, for typical wavelengths in the visible range used in light scattering experiments (e.g., 514.5 or 632.8 nm), primary particle size parameter $x = \pi d/\lambda$ is comfortably below 0.4.

RESULTS AND DISCUSSION

The following questions will be analyzed throughout the present section: i) what should be a reference value for the fractal prefactor, k_g, of cluster–cluster aggregates? ii) experimental predictions of k_g can exceed numerical results by more than 100%. To what degree are both predictions correct? Can experimental and numerical results be correlated?

Evaluation of the Fractal Dimensions of "Free" Cluster–Cluster Aggregates

To establish a reference value for the fractal dimension and prefactor, a large population of cluster–cluster aggregates was generated without imposing any restrictions on the fractal properties (presently denoted as "free" aggregates). As seen in Figure 1, results obtained for this population of 256 aggregates having $N = 8 - 1024$ satisfy the power–law relationship of Equation (1) with D_f ca. 1.88 and k_g roughly 1.45. These results are in very good agreement with several independent numerical predictions reported by previous authors; see Table 1. However, they only suggest that our numerically simulated aggregates exhibit fractal concepts. They do not guarantee that these fractal results should become a reference. To confirm the validity of these predictions, we have investigated what these variables would be when inferred from laser light scattering predictions.

As previously mentioned, fractal theories suggest that the slope of C_{vv} versus qa in a log–log plot in the large angle regime should be equal to $-D_f$. We have calculated this slope using the IEFS formulation for the present population of aggregates. Thirty-two different

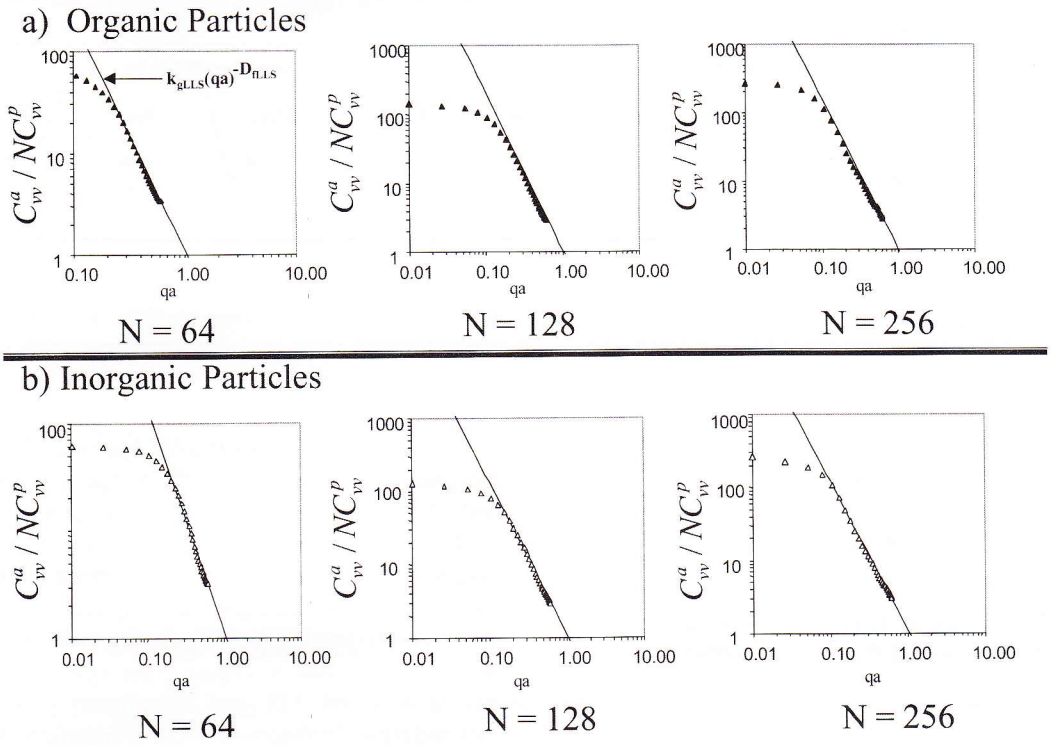

FIGURE 2. Normalized *vv* differential scattering cross sections as a function of the radiation momentum, *qa*, for "free" simulated aggregates having $N = 64$, 128, and 256 using IEFS theory ($\lambda = 514.5$ nm, $x_p = 0.4$); a) $m = 1.57 + 0.57I$; and b) $m = 0.7 + 0i$).

realizations of the same aggregate size, each sampled at 16 different orientations, were averaged to obtain statistically significant IEFS predictions with <10% numerical uncertainties (95% confidence interval).

Results obtained for aggregate size classes having $N = 64$, 128, and 256 are shown in Figure 2. Two types of aggregates were considered. Organic combustion generated particles (e.g., soot) with a complex refractive index $m = 1.56 + 0.56i$ and inorganic nonabsorbing particles (such as alumina) with $m = 1.7$. Calculations were performed using a typical wavelength employed in light scattering experiments ($\lambda = 514.5$ nm) and a primary particle within the range that usually characterizes these nanosize particles ($a = 50$ nm). These values lead to a primary particle size parameter $x = \pi d/\lambda = 0.3$ and are therefore within the range of validity of the IEFS theory (Farias et al. 1996).

Unfortunately, the values obtained for the fractal dimensions, D_{fLLS} and k_{gLLS}, are not very similar to the ones obtained using the morphological fractal concept based on Equation (1). Table 2 includes the results obtained using these two techniques for comparison. It appears that the fractal dimension obtained through light scattering consistently overestimates results based on the radius of gyration. On the contrary, the fractal prefactor deviations are in the order of 20–30%, clearly outside the uncertainties of the present predictions. Results obtained also seem to be fairly insensitive to aggregate size and composition, at least within the range of number of primary particles, N, and complex refractive indices considered.

TABLE 2. Fractal dimension and fractal prefactor for "free" simulated aggregates using light scattering and morphological predictions.

	Organic Particles				Inorganic Particles			
N	k_{gLLS}	D_{fLLS}	k_{gM}	D_{fM}	k_{gLLS}	D_{fLLS}	k_{gM}	D_{fM}
64	1.10	2.30	1.44	1.89	1.15	2.10	1.44	1.89
128	1.05	2.30	1.44	1.89	1.10	2.10	1.44	1.89
256	1.05	2.20	1.44	1.89	1.10	2.05	1.44	1.89

The question to be raised now is as follows: would aggregates having a morphological fractal prefactor different from our estimates based on "free" simulations (i.e., $k_g > 1.45$ or <1.45) perform in a different way? In particular, could they exhibit a better agreement between light scattering and morphological predictions? This issue will be addressed in the next section.

Evaluation of Aggregates Having Preestablished Fractal Properties

One advantage of the model used in the present work to simulate aggregates is the possibility of selecting the morphological fractal properties desired for the population. The control of these properties is done during the construction of the aggregate. To be more precise, when two clusters are attached, the radius of gyration of the new cluster is calculated based on the known positions of the primary particles and Equation (1) is checked to see if it is satisfied for the fractal dimension and prefactor selected. This step guarantees that the final aggregate (as well as each intermediate cluster) will have the appropriate fractal dimensions. This possibility was used in the present work to investigate two families of aggregates, one having $k_g > 2$ and another with k_g ca. 1 (representing the lower limit of the values shown in Table 1). In both cases D_f was selected to fall in the range of 1.7–1.9 as predicted by the majority of researchers (see Table 1). The morphological fractal dimension and fractal prefactor of these simulated aggregates resulted from log–log plots of N versus radius of gyration (similar to Figure 1). However, in these cases, aggregates perfectly satisfy Equation (1)—a direct consequence of the numerical procedure adopted—and therefore the plots (not shown) were almost perfect straight lines.

Population of Aggregates Having $k_{gM} > 2$. Our morphological calculation indicate $k_{gM} = 2.23$ and D_{fM} of 1.81. This comes as no surprise as they were forced while constructing the aggregates. Therefore, a way of confirming their validity is through the light scattering prediction in the power–law regime. Results for these predictions are shown in Figure 3 for aggregates having $N = 64$, 128, and 256 primary particles and typical refractive indices of organic and inorganic particles. Fractal properties inferred from these plots are summarized in Table 3. The fractal dimension inferred from the power–law slope systematically overestimates the preestablished value of 1.81. This tendency is general for all situations considered with deviations falling in the range of 20–40%. The fractal prefactor predictions exhibit even larger deviations. Light scattering predictions indicate k_{gLLS} ca. 1.0–1.4, while the morphological value defined is 2.23, i.e., roughly 100% more. These results have been observed in the past by Farias et al. (1995) when investigating the validity of light scattering theories for soot aggregates. In summary, there is a clear lack of consistency between morphological and light scattering predictions indicating that large values of k_g based on Equation (1) appear to be incapable of satisfying independent characteristics of fractals.

Population of Aggregates Having k_{gM} ca. 1. The opposite scenario is now considered: A population of aggregates having $k_{gM} = 1.0$ and

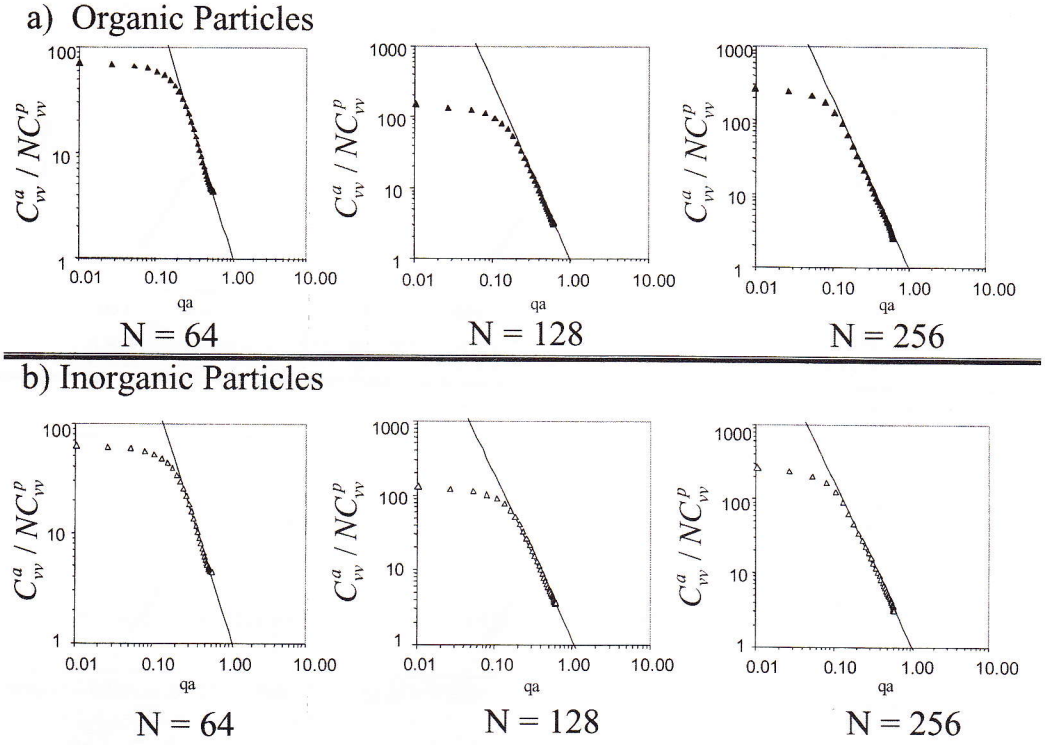

FIGURE 3. Normalized *vv* differential scattering cross sections as a function of the radiation momentum, *qa*, for simulated aggregates having preestablished morphological fractal dimensions $k_g > 2$ and $D_f = 1.7$–1.9.

$D_{fM} = 1.8$ is now taken into consideration. Following the same procedure, we have estimated the fractal properties inferred from light scattering predictions and compared with the preestablished morphological values. Figure 4 shows the light scattering results obtained for the same aggregate sizes and refractive indices. Values extracted from these plots are summarized in Table 4. The opposite tendencies are now verified, i.e., the fractal dimensions, D_f, estimated from light scattering predictions, slightly underestimate the predefined morphological value. Deviations are very small (ca. 5%) and within our numerical uncertainties. The fractal prefactor, k_g, is now roughly 25–50% above the predefined value of 1.

From the results presented so far it appears that there should be a specific value of k_g where

TABLE 3. Fractal dimension and fractal prefactor for simulated aggregates having preestablished morphological fractal dimensions ($k_{gM} = 2.23$ and $D_{fM} = 1.7$–1.9).

	Organic Particles				Inorganic Particles			
N	k_{gLLS}	D_{fLLS}	k_{gM}	D_{fM}	k_{gLLS}	D_{fLLS}	k_{gM}	D_{fM}
64	1.20	2.35	2.23	1.81	1.30	2.20	2.23	1.81
128	0.95	2.50	2.23	1.81	1.20	2.20	2.23	1.81
256	0.95	2.30	2.23	1.81	1.10	2.20	2.23	1.81

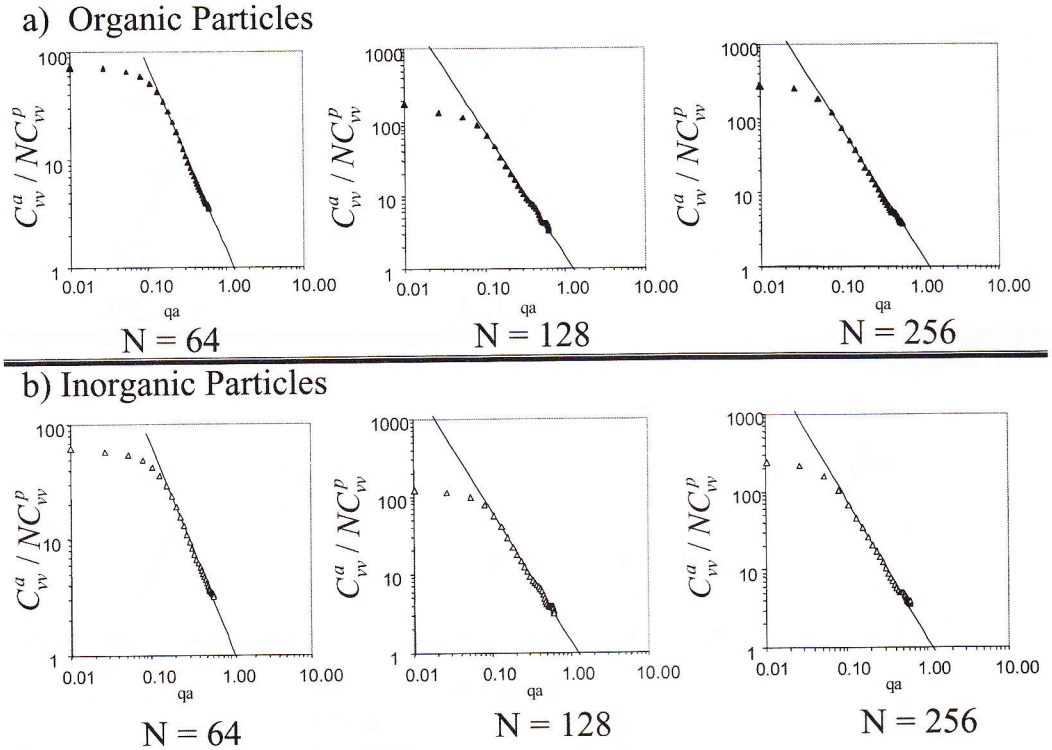

FIGURE 4. Normalized *vv* differential scattering cross sections as a function of the radiation momentum, *qa*, for simulated having preestablished morphological fractal dimensions $k_g \approx 1$ and $D_f = 1.7$–1.9.

both morphological and light scattering predictions would match. In order to investigate this value, Figures 5 and 6 summarize the results obtained for the fractal dimensions using the two methods adopted in the present work. Included in those figures are trend lines as well as the line where both values would match. From these plots, our best estimates suggest $k_g = 1.27 \pm 0.1$ and $D_f = 1.82 \pm 0.05$. To make a final confirmation of these values we have generated a population of aggregates having $k_{gM} \approx 1.26$ and $D_{fM} \approx 1.8$ and compared these predefined values with light scattering predictions. Results obtained ($k_{gLLS} = 1.3$ and $D_{fLLS} = 1.84$) were very consistent leading to deviations of <5% and 3%, respectively, i.e., within our numerical uncertainties. These values are very similar to the ones presented by Wu and Friedlander

TABLE 4. Fractal dimension and fractal prefactor for simulated aggregates having preestablished morphological fractal dimensions ($k_{gM} \approx 1$ and $D_f = 1.7$–1.9).

	Organic Particles				Inorganic Particles			
N	k_{gLLS}	D_{fLLS}	k_{gM}	D_{fM}	k_{gLLS}	D_{fLLS}	k_{gM}	D_{fM}
64	1.50	1.70	1.02	1.80	1.24	1.80	1.02	1.80
128	1.50	1.70	1.02	1.80	1.39	1.78	1.02	1.80
256	1.60	1.70	1.02	1.80	1.28	2.80	1.02	1.80

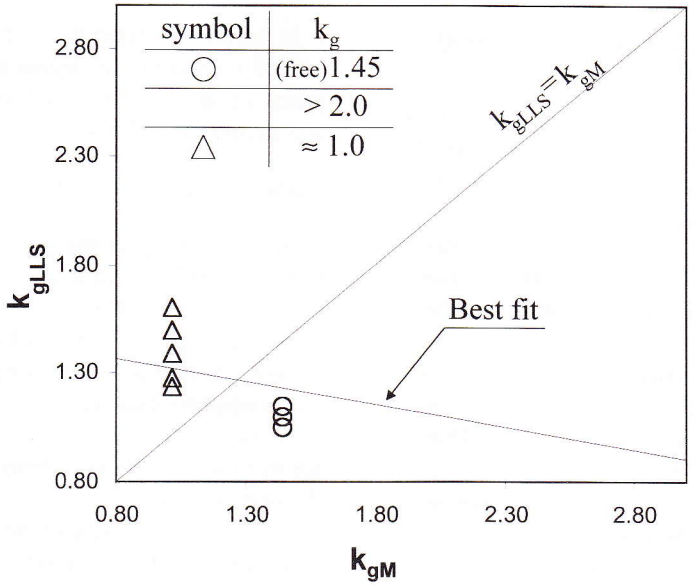

FIGURE 5. k_g **predictions resulting from morphological analysis (k_{gM}) and Laser Light Scattering predictions (k_{gLLS}).**

(1993), Mountain et al. (1986), and Mulholland and Mulholland (1988); which were all obtained from computer simulated aggregates. They also follow very closely the experimental predictions reported by Cai et al. (1995); see Table 1. Apart from this exception, our predictions are consistently smaller than the ones based on experimental results. Potential reasons for these discrepancies are discussed in the following section.

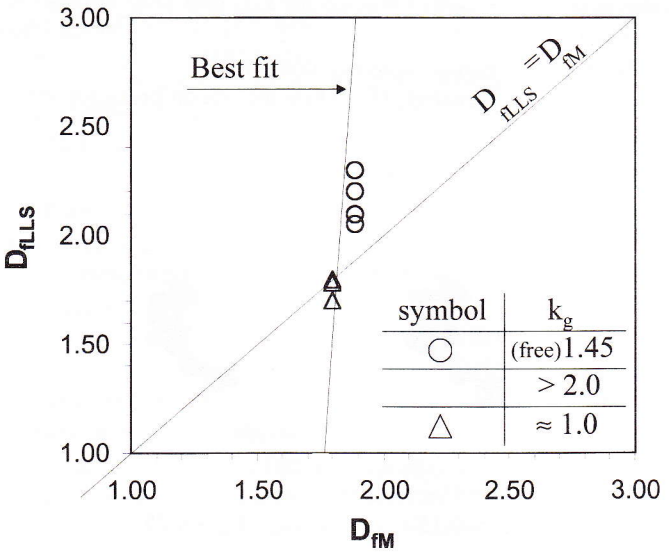

FIGURE 6. D_f **predictions resulting from morphological analysis (D_{fM}) and Laser Light Scattering predictions (D_{fLLS}).**

Evaluation of the Fractal Dimensions of Aggregates with Partial Sintering

One pertinent question that may arise is related to the systematic gap between the numerical and experimental predictions of the fractal dimensions. In particular, why do results published for k_g based on real aggregates (e.g., soot, silica, or alumina) tend to over predict numerical estimates? One possible reason is the cutoff function coefficient that is >1.5 for typical polydisperse combustion generated aggregates but has been consistently ignored (which means imposing the k_p values = 1). An addition or completely possible reason is analyzed below.

Most numerical models that simulate agglomerates of spherical particles assume that neighboring monomers touch on a single point. Real aggregates do not satisfy this theoretical condition. In fact, there are several different physical and environmental effects that contribute to a certain degree of penetration leading to more compact and rigid aggregates, namely, strong attraction forces between particles, lack of rigidity of the particle matter, aggregates crossing high temperature environments, or the impact between the monomers when attaching to each other. Thus, one possible reason for this problem is the fact that in real aggregates neighboring particles do not just touch each other, i.e., a certain degree of penetration occurs between touching particles.

In the present paper the term partial sintering will be related to this degree of penetration of primary particles. A penetration coefficient, C_p, was defined as follows:

$$C_p(\%) = (d_p - d_{ij})/(d_p), \tag{7}$$

where d_{ij} represents the distance between two touching particles while d_p is the diameters of primary particles. If $C_p = 0$, the primary particles are in point contact while $C_p = 1$ total sintering took place, indicating that every couple of neighbors merged into a single particle.

Numerically, partial sintering was accounted for by progressively increasing the diameters of the primary particles within an aggregate while maintaining the position of the center of the particle, followed by a scaling correction to keep the same reference value for particle diameter. In Figure 7, projected images of a numerically simulated aggregate having $N = 64$ and $C_p = 0$, 0.15, and 0.25 are shown. This figure highlights the effect of partial sintering on the aggregate size, compactness, and, more important, radius of gyration.

Figure 8 shows a log–log plot of R_g/a versus N for the population of aggregates generated (with the different degrees of partial sintering). Results obtained for k_{gM} and D_{fM} are also included in Figure 8. It is interesting to note that partial sintering does not affect the fractal dimension, D_f, while the fractal prefactor varies

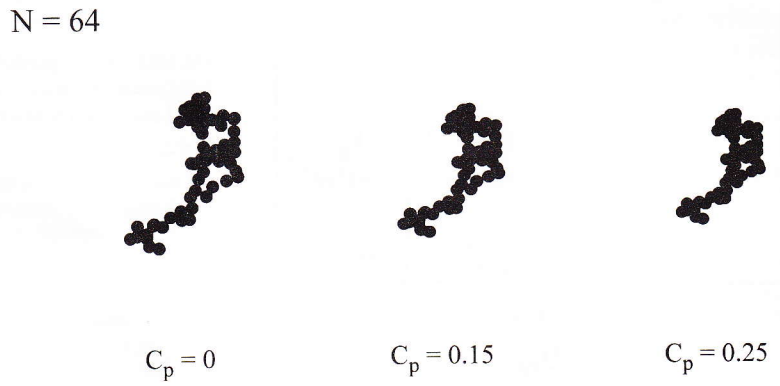

FIGURE 7. Projected image of a typical simulated aggregate having $N = 64$ and $C_p = 0$, 0.15, and 0.25.

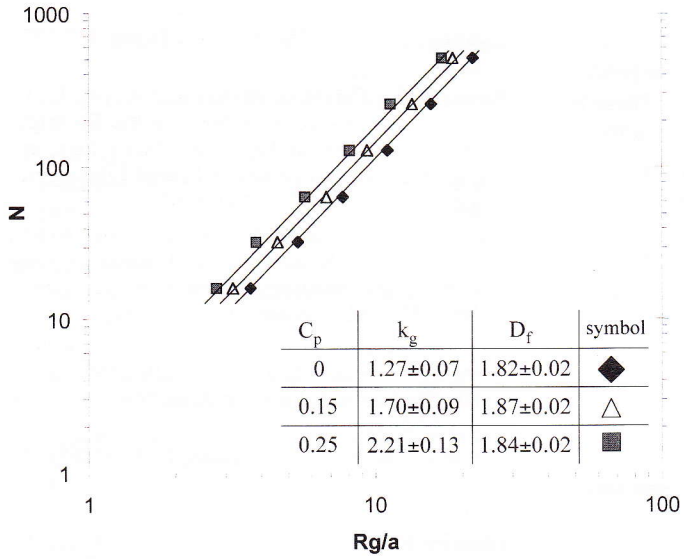

FIGURE 8. Number of particles per aggregate versus radius of gyration normalized by particle radius for simulated aggregates with different penetration coefficients, C_p.

by more than a factor of 2. From the present results it can be concluded that a penetration coefficient of 15–20% increases k_g to values relatively closer to the experimental results reported by several independent authors (i.e., >2). It is interesting to see that the only experimental predictions that match our numerical conclusions belong to Cai et al. (1995). Relevant (or not) to this comparison, their aggregates were generated from a methane oxygen enriched flame while the remaining authors—namely, Köylü et al. (1995a), Puri et al. (1993), and Megaridis and Dobbins (1990)—used either acetylene or ethylene nonpremixed flames, i.e., heavy sooting flames. It would be interesting to compare the morphology, in particular, the differences of partial sintering that may exist between these aggregates.

In summary, partial sintering that occurs between neighboring particles may be responsible for the systematic gap between experimental and numerical results reported for k_g. This effect can be complimented by the fact that real aggregate populations are polydisperse and therefore have a cut-off function coefficient, k_p, >1. However, it is clear that these results are insufficient to outline any definitive conclusions. Additional studies regarding the high experimental value for k_g should be foreseen.

CONCLUSIONS

The main conclusions of the present study can be summarized as follows:

1. Results obtained for "free" simulated aggregates (i.e., without restricting the fractal dimensions) are in agreement with several independent results reported by previous authors, namely, $k_{gM} = 1.45$ and D_{fM} ca. 1.89. However, light scattering prediction of k_g and D_f are inconsistent with these morphological values.
2. Aggregates having predefined values for $k_g > 2$ as proposed by most experimental studies exhibit light scattering curves that are even more inconsistent with fractal concepts.
3. Our suggestions for the fractal properties (D_f and k_g) of simulated cluster–cluster aggregates were obtained from a best fit between the results obtained for the different populations of aggregates considered (i.e., having $k_g \approx 1.0$, 1.45, and 2.2 and $D_f = 1.82$).

Best estimates are $k_g \approx 1.27$ and $D_f \approx 1.82$, which seem to be approximately independent of aggregate size and composition. These results are in very good agreement with results reported by Wu and Friedlander (1993), Mountain et al. (1986), and Cai et al. (1995), among others.

4. Finally, partial sintering that unavoidably occurs between neighboring particles of aggregates appears to contribute to a systematic increase in k_g, while keeping D_f approximately constant. This effect, complimented by the fact that real aggregate populations are polydisperse (having a cut-off function coefficient, $k_p, >1$) may justify the differences usually found between numerical and experimental results reported in the literature for k_g.

A. M. Brasil would like to acknowledge the scholarship of Conselho Nacional de Desenvolvimento Científico e Tecnológico—CNPq.

References

Berry, M. V., and Percival, I. C. (1986). Optics of Fractal Clusters Such as Smoke, *Optica Acta*. 33:577–591.

Botet, R., and Jullien, R. (1988). A Theory of Aggregating Systems of Particles: The Clustering of Clusters Process, *Ann. Phys. Fr.* 13:153.

Brasil, A. M., Farias, T. L., and Carvalho, M. G. (1999). A Recipe for Image Characterization of Fractal-Like Aggregates, *J. Aerosol Sci.*, in press.

Cai, J., Lu, N., and Sorensen, C. M. (1995). Analysis of Fractal Cluster Morphology Parameters: Structural Coefficient and Density Autocorrelation Function Cutoff, *J. Colloid Interface Sci.* 171:470–473.

Dobbins, R. A., and Megaridis, C. M. (1991). Absorption and Scattering of Light by Polydisperse Aggregates, *Appl. Optics*. 30:4747–4754.

Draine, B. T. (1988). The Discrete-Dipole Approximation and Its Application to Interstellar Graphite Grains, *Astrophysical Journal* 333:848–872.

Farias, T. L., Carvalho, M. G., Köylü, Ü. Ö., and Faeth, G. M. (1995). Computational Evaluation of Approximate Rayleigh-Debye-Gans/Fractal-Aggregate Theory for the Absorption and Scattering Properties of Soot, *J. Heat Transf.* 117:152–159.

Farias, T. L., Carvalho, M. G., and Köylü, Ü. Ö. (1996). The Range of Validity of the Rayleigh-Debye-Gans/Fractal-Aggregate Theory for Computing Optical Properties of Fractal-Like Aggregates, *Appl. Optics* 35:6560–6567.

Farias, T. L., Carvalho, M. G., and Köylü, Ü. Ö. (1998). Radiative Heat Transfer in Soot-Containing Combustion System with Aggregation, *Int. J. Heat Mass Tranf.* 41:2581–2587.

Goedecke, G. H., and O'Brien, S. O. (1988). Scattering by Irregular Inhomogeneous Particles via the Digitized Green's Function Algorithm, *Appl. Optics* 27:2431–2438.

Hutchison, H. P., and Sutherland, D. N. (1965). An open-structured random solid, *Nature* 206:1036–1037.

Iskander, M. F., Chen, H. Y., and Penner, J. E. (1989). Optical Scattering and Absorption by Branched Chains of Aerosols, *Appl. Optics* 28:3083–3091.

Jones, A. R. (1979a). Electromagnetic Wave Scattering by Assemblies of Particles in the Rayleigh Approximation, *Proc. Roy. Soc. London* 366:111–127.

Jones, A. R. (1979b). Scattering Efficiency Factors for Agglomerates of Small Spheres, *J. Phys. D: Appl. Phys.* 12:1661–1672.

Jullien, R., and Botet, R. (1987). *Aggregation and Fractal Aggregates*, World Scientific Publishing Co., Singapore, pp. 46–60.

Köylü, Ü. Ö., and Faeth, G. M. (1992). Structure of Overfire Soot in Buoyant Turbulent Diffusion Flames at Long Residence Times, *Combust. Flame* 89:140–156.

Köylü, Ü. Ö., and Faeth, G. M. (1994a). Optical Properties Soot in Buoyant Turbulent Diffusion Flames at Long Residence Times, *J. Heat Trans.* 116:152–159.

Köylü, Ü. Ö., and Faeth, G. M. (1994b). Optical Properties of Soot in Buoyant Laminar Diffusion Flames at Long Residence Times, *J. Heat Trans.* 116:971–979.

Köylü, Ü. Ö., Faeth, G. M., Farias, T. L., and Carvalho, M. G. (1995b). Fractal and Projected Structure Properties of Soot Aggregates, *Combust. Flame* 100:621–633.

Köylü, Ü. Ö., McEnally, C. S., Rosner, D. E., and Pfefferle, L. D. (1997). Simultaneous Measurements of Soot Volume Fraction and Particle Size/Microstructure in Flames Using a Thermophoretic Sampling Technique, *Comb. Flame* 110:494–507.

Köylü, Ü. Ö., Xing, Y., and Rosner, D. E. (1995a). Fractal Morphlogy Analysis of Combustion-Generated Aggregates Using Angular Light Scattering and Electron Microscope Images, *Langmuir* 11:4848–4854.

Lou, W., and Charalampopoulos, T. T. (1994). On the Electromagnetic Scattering and Absorption of Agglomerated Small Spherical Particles, *J. Physics D: Appl. Phys.* 27:2258–2270.

Meakin, P. (1983a). Diffusion Controlled Cluster Formation in Two, Three, and Four Dimensions, *Physical Review A* 27:604–607.

Meakin, P. (1983b). Diffusion Controlled Cluster Formation in 2-6-Dimensional Space, *Physical Review A* 27:1495–1507.

Meakin, P. (1984). Diffusion-Limited Aggregation in Three Dimensions: Results from a New Cluster-Cluster Aggregation Model, *J. Colloid Interface Sci.* 102:491–504.

Megaridis, C. M., and Dobbins, R. A. (1990). Morphological Description of Flame-Generated Materials, *Combust. Sci. Tech.* 71:95–109.

Mountain, R. D., Mulholland, G. W., and Baum, H. (1986). Simulation of Aerosol Agglomeration in the Free Molecular and Continuum Flow, *J. Colloid Interface Sci.* 114:67–81.

Mountain, R. D., and Mulholland, G.W. (1988). Light Scattering from Simulated Smoke Agglomerates, *Langmuir* 4:1321–1326.

Nelson, J. (1989). Test of a Mean Field Theory for the Optics of Fractal Clusters, *J. Modern Optics* 36:1031–1057.

Oh, C., and Sorensen, C. M. (1997). The Effect of Overlap Between Monomers on the Determination of Fractal Cluster Morphology, *J. Colloid Interface Sci.* 193:17–25.

Oh, C., and Sorensen, C. M. (1998). The Structure Factor of Diffusion-Limited Aggregation Clusters: Local Structure and Non-Self-Similarity, *Physical Review E.* 57:784–790.

Purcell, E. M., and Pennypacker, C. R. (1973). Scattering and Absorption of Light by Nonspherical Dielectric Grains, *Astrophys J.* 186:705–714.

Puri, R., Richardson, T. F., Santoro, R. J., and Dobbins, R. A. (1993). Aerosol Dynamic Processes of Soot Aggregates in a Laminar Ethene Diffusion Flame, *Combust. Flame* 92:320–333.

Samson, R. J., Mulholand, G. W., and Gentry, J. W. (1987). Structural Analysis of Soot Agglomerates, *Langmuir* 3:272–281.

Saxon, D. S. (1974). Lectures on the Scattering of Light. *The UCLA International Conference on Radiation and Remote Probing of the Atmosphere*, edited by J. G. Kuriyan, pp. 227–308.

Sorensen, C. M., and Roberts, G. C. (1997). The Prefactor of Fractal Aggregtes, *J. Colloid Interface Sci.* 186:447–452.

Sorensen, C. M., and Wang, G. M. (1999). Size Distribution Effect on the Power Law Regime of the Structure Factor of Fractal Aggregtes, *Phys. Rev. E*, in press.

Vold, M. J. (1963). Computer Simulation of Floc Formation in a Colloidal Suspension, *J. Colloid Sci.* 18:684–695.

Witten, T. A., and Sander, L. M. (1981). Diffusion-Limited Aggregation, A Kinetic Critical Phenomenon, *Phys. Rev. Lett.* 47:1400–1403.

Witten, T. A., and Sander, L. M. (1983). Diffusion-Limited Aggregation, *Phys. Rev. B.* 27:5685–5697.

Wu, M., and Friedlander, S. K. (1993). Note on the Power-Law Equation for Fractal-Like Aerosol Agglomerates, *J. Colloid Interface Sci.* 159:246–248.

NOMENCLATURE

a	primary particle radius;
C_p	penetration coefficient;
C_{vv}^a	vertical–vertical differential scattering cross section of an aggregate;
C_{vv}^p	vertical–vertical differential scattering cross section of a primary particle;
D_f	aggregate fractal dimension;
D_{fM}	morphological fractal dimension;
D_{fLLS}	laser light scattering fractal dimension;
d_p	primary particle diameter;
k_g	fractal prefactor;
k_{gM}	morphological fractal prefactor;
k_{gLLS}	laser light scattering fractal prefactor;
k_p	cut-off function coefficient;
m	complex refractive index ($m = n + i\kappa$);
N	number of primary particles in an aggregate;
q	modulus of the scattering vector;
R_g	radius of gyration of an aggregate;
x_p	primary particle size parameter, $\pi d_p/\lambda$.

Greek Symbols

λ	wavelength;
θ, ϕ	coordinates of the scattered field.

Received August 2, 1999; accepted January 3, 2000.